





## Article

# Optimization of the Application of Commercial Hydrophobic Coatings for Natural Stone Protection and Preservation

Hurraira Hashim<sup>1</sup>, Luís Dias<sup>1,2</sup>, Sérgio Martins<sup>1,2</sup> , Vera Pires<sup>1,2,3</sup> , Mafalda Costa<sup>1,2</sup>  and Pedro Barrulas<sup>1,2,4,\*</sup> 

<sup>1</sup> HERCULES Laboratory, University of Évora, Palácio do Vimioso, Largo Marquês de Marialva 8, 7000-809 Évora, Portugal; hurraira4065@gmail.com (H.H.); luisdias@uevora.pt (L.D.); smam@uevora.pt (S.M.); vlcp@uevora.pt (V.P.); mcosta@uevora.pt (M.C.)

<sup>2</sup> Associate Laboratory for Research and Innovation in Heritage, Arts, Sustainability and Territory IN2PAST, Évora University, Largo Marquês de Marialva 8, 7000-809 Évora, Portugal

<sup>3</sup> Laboratory of Mechanical Tests (LEM), School of Science and Technology, University of Évora, Colégio Luís António Verney, R. Romão Ramalho 59, 7000-671 Évora, Portugal

<sup>4</sup> Department of Chemistry and Biochemistry, School of Science and Technology, University of Évora, Colégio Luís António Verney, R. Romão Ramalho 59, 7000-671 Évora, Portugal

\* Correspondence: pbarrulas@uevora.pt

**Abstract:** Natural stone has been used worldwide in the construction of archaeological and historical heritage. However, its preservation continues to be threatened by weathering and degradation phenomena. Water is widely recognized as the most threatening external component that contributes to stone deterioration, increasing the need for the development of protective hydrophobic coatings to eliminate water penetration. This study intends to contribute to the better understanding of natural stone treatment strategies to prevent water penetration and subsequent stone alteration by studying the effect of coating and stone substrate temperatures, and the number of coating applications, on the effectiveness, compatibility, and durability of commercial hydrophobic coatings. The results obtained revealed that while more than one application increases coating hydrophobic effectiveness, it frequently leads to changes in the aesthetic appearance of natural stone, including whitening and darkening of the substrate's original hues. Improved hydrophobic effectiveness (maximum gain of  $\approx 9\%$ ) is also achieved when applying the commercial coatings at 4 °C to natural stone substrates maintained at room temperature, conditions that are feasible to be used in real life. Additionally, the commercial coating composed of silane/siloxane with modified fluorinated additives was found to be the most effective and durable hydrophobic solution.

**Keywords:** natural stone; stone deterioration; hydrophobic coatings; built heritage; conservation



**Citation:** Hashim, H.; Dias, L.; Martins, S.; Pires, V.; Costa, M.; Barrulas, P. Optimization of the Application of Commercial Hydrophobic Coatings for Natural Stone Protection and Preservation. *Heritage* **2024**, *7*, 3495–3510. <https://doi.org/10.3390/heritage7070165>

Academic Editors: Anna Klisińska Kopacz and Anna Ryguła

Received: 9 May 2024

Revised: 24 June 2024

Accepted: 27 June 2024

Published: 1 July 2024



**Copyright:** © 2024 by the authors. Licensee MDPI, Basel, Switzerland. This article is an open access article distributed under the terms and conditions of the Creative Commons Attribution (CC BY) license (<https://creativecommons.org/licenses/by/4.0/>).

## 1. Introduction

Natural stone has been widely used in construction since around 10,000 BC, based on the discovery of well-defined stone-lined structures in the Mediterranean Levantine region dated to as early as the end of the Epipaleolithic (10.550–8.350 BC) [1] and the earliest architectural stone structures found in Anatolia dated to the Later Pre-Pottery Neolithic A period [2]. More expensive than its counterparts wood and earth materials, natural stone usage was (and still is) influenced by socio-economical aspects, but also by its physical–chemical and mechanical properties, which dictate perceived beauty but also its durability [3]. Additionally, natural stone is considered a sustainable and green building material due to its low energy consumption during processing, significant recyclability, and circular economy applications [4]. However, it is crucial to consider the transportation distance from the quarry to the construction site. If the stone is sourced from a location far from its intended use, the environmental impact of transporting the heavy material, which involves substantial fuel consumption and greenhouse gas emissions, along with

the associated costs, can negate many of the sustainability advantages. Therefore, sourcing natural stone locally or from nearby regions is essential to maximizing its eco-friendly benefits and minimizing the carbon footprint associated with long-distance transport [5]. This versatility makes natural stone an excellent resource for both interior and exterior architectural structures [1,4,6]. However, it is prone to weathering and deterioration, which threatens the preservation of archaeological and historical built heritage recognized for its cultural significance globally [1,7,8]. The main causes of natural stone deterioration include air pollution, the presence of soluble salts, and biocolonization [8–10]. All of these deterioration mechanisms have one common factor: water [10,11]. Water facilitates the dissolution and movement of soluble salts within the stone, leading to efflorescence and salt-induced spalling. It also acts as a solvent for gaseous contaminants that can chemically attack the stone [8,9]. Additionally, water within the stone's pores can compromise its mechanical resistance, particularly through freeze–thaw cycles that cause pore expansion and contraction [12]. Preventing water penetration is therefore crucial for mitigating natural stone deterioration and contributing to its preservation.

The protection of natural stone, particularly in cultural heritage contexts, presents a complex challenge. This has led to the development of various hydrophobic coatings designed to repel moisture and rainwater while maintaining stone breathability to prevent damage from trapped water within the substrate [13–15].

Many of the coatings used in the preservation of natural stone were designed for industrial applications on other materials [16]. Previous studies have extensively explored various hydrophobic coatings for natural stone preservation. For instance, acrylic and vinyl polymers have been traditionally used due to their film-forming abilities, but they face issues related to breathability, long-term stability, irreversible molecular modifications, and loss of conservative properties. Organosilicone compounds have shown better performance in terms of water repellency and breathability, but their application can be affected by substrate compatibility and environmental conditions [16]. More recently, novel hybrid coatings have been developed to protect natural stone against deterioration caused by water, pollutants, and biological activity [17]. These hybrid solutions combine organic and inorganic components, such as acrylics and siloxanes, with nano-oxides (e.g., silica, alumina, tin oxide, and titania), to create colorless, self-cleaning treatments for natural stone [17–20]. However, long-term stability in terms of water repellency and coating adhesion, mechanical and physical durability, and color/reflectance compatibility still pose important challenges when hydrophobic coatings are applied to natural-stone-built heritage.

This study aims to determine the effect of application procedures, specifically coating and substrate temperatures, and the number of coating applications, on the effectiveness, compatibility, and durability of different hydrophobic coatings for natural stone. By investigating these variables, we aim to improve the application methods and performance of hydrophobic coatings in preserving stone-built heritage.

## 2. Materials and Methods

### 2.1. Materials

#### 2.1.1. Natural Stone Mock-Ups

Three commercially valuable natural stones—a limestone with open porosity of 8.50%, a marble with open porosity of 0.20%, and a granitoid with open porosity of 0.60%—all quarried in Portuguese territory, were selected to serve as stone substrates in this study. These three different lithotypes were selected to ensure that the coatings were applied on surfaces with distinct physical–chemical properties (Table 1) and on natural stones frequently used in Portuguese built heritage from pre-historic monumental megalithic structures to modern and contemporary buildings.

Mock-ups of the natural stone lithotypes were wet cut to have  $30 \times 30 \times 4$  mm dimensions using a cutting saw (Struers, Copenhagen, Denmark), using the same procedure described by Armal et al. [10]. These natural stone mock-ups were then washed with

distilled water and dried at 60 °C in the oven before being analyzed using the multi-analytical approach described below.

**Table 1.** Average physical–mechanical properties of the selected lithotypes [21].

Property	Limestone (L)	Marble (M)	Granitoid (G)
Bulk density [kg/m <sup>3</sup> ]	2393 ± 7	2714 ± 6	2722 ± 5
Open porosity [%]	7.8 ± 0.2	0.4 ± 0.02	0.05 ± 0.01
Water absorption at atmospheric pressure [%]	3.0 ± 0.5	0.1 ± 0.02	0.1 ± 0.01
Water absorption by capillarity [g/m <sup>2</sup> ·s <sup>0.5</sup> ] (Parallel to bedding plane/perpendicular to bedding plane)	30/13	0.9/0.8	0.7/0.6
Compressive uniaxial strength [MPa]	75 ± 6	85 ± 6	150 ± 7
Flexural strength under concentrated load [MPa]	11.1 ± 0.6	16.4 ± 3	16.9 ± 2

### 2.1.2. Commercial Hydrophobic Coatings

Three commercial hydrophobic coatings named Coating Number 1 (CN1), Coating Number 2 (CN2), and Coating Number 3 (CN3) were applied on the surface of the different natural stone lithotypes. As authorization has not been granted to reveal the true marketing names of these coatings, only their chemical compositions will be provided. CN1 is a whitish, highly alkaline, aqueous solution of Potassium Methyl Siliconate (PMS), which has a drying time of 12–24 h. CN2 is a colorless/transparent, VOC-free (free of volatile organic compounds) solution of fluorocarbon polymer, which has the same drying time as CN1. CN3 is a VOC-free milky solution of silanes/siloxanes with modified fluorinated additives, whose drying time is similar to that of CN1 and CN2.

Prior to their application, each coating was prepared according to the requirements provided by their respective manufacturing company. CN1 and CN2 were ready for use without any dilution, while CN3 was prepared by diluting with distilled water in a 1:9 ratio.

## 2.2. Methodology

### 2.2.1. Coating Application

The spray-coating technique was employed to apply the three commercial hydrophobic solutions (CN1, CN2, and CN3) on the natural stone substrates. The spray-coating technique provides a versatile, fast, and economical solution for producing large superhydrophobic surfaces, offering advantages like simplicity, automation, and cost-effectiveness [22].

A spray gun and a Michelin MB24 air compressor running on 230 V, with a sucked air flow of 170 L/min and with a maximum pressure of 8 bar, were employed to create the fine mist of coating solution dispersed through the spray gun nozzle. A total of 20 mL of solution of each commercial coating was applied using an application time of 2 s and maintaining a working distance of approximately 1 m between the natural stone substrates and the spray-gun nozzle. The coated natural stone lithotypes were placed horizontally and dried at room temperature (25 °C) for 12 to 24 h, using the recommended drying time provided by the manufacturing company of each commercial coating.

In order to study the effect of coating and natural stone substrate temperatures, and the number of coating applications, on the effectiveness, compatibility, and durability of the three commercial hydrophobic coatings, these application parameters were tested, as illustrated in Figure 1. The performance of the hydrophobic coatings was subsequently measured to determine the optimal parameters of the hydrophobic coating application, which can be adopted consistently in real-life conditions.

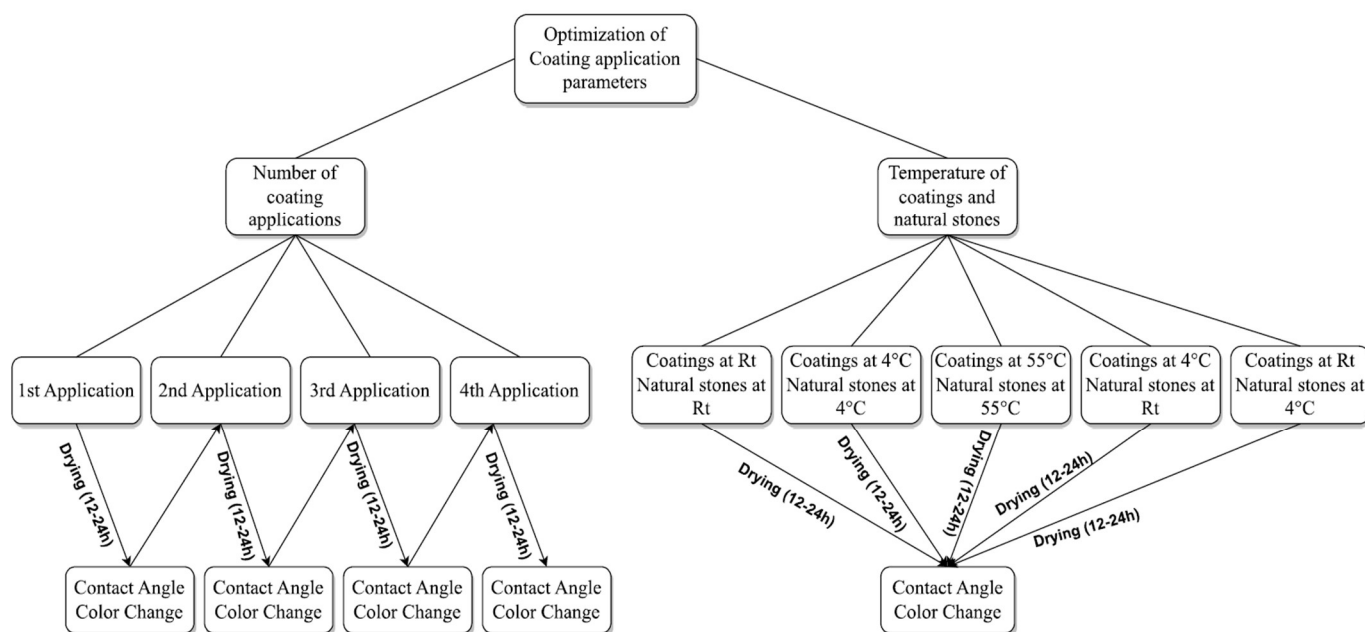


**Figure 1.** Optimization of coating application. Rt stands for room temperature.

### 2.2.2. High-Resolution Digital Microscopy

A HRX-01 microscope (HIROX, Tokyo, Japan) was used to capture high-resolution images of the natural stone mock-ups before and after the application of the commercial hydrophobic coatings and after accelerated ageing, in order to document and assess the presence of aesthetic changes caused by the coatings' deposition and deterioration. This enabled the determination of the aesthetic compatibility of the coatings (CN1, CN2, and CN3) with the natural stone substrates.

### 2.2.3. Scanning Electron Microscopy Coupled to Energy-Dispersive X-ray Spectroscopy (SEM–EDS)

A variable-pressure HITACHI S3700N SEM coupled with a Quantax EDS micro-analysis system was used to characterize the coated natural stone lithotypes and gain a comprehensive insight into their surface morphology. A Bruker AXS XFlash® Silicon Drift Detector (<129 eV Spectral Resolution at FWHM/MnK $\alpha$ ) was used in the Quantax Compact Plus 30 system. The Bruker ESPRIT Compact software (ver. 2.3.1.109) was used to acquire data and perform a standardless PB/ZAF semi-quantitative elemental analysis. Backscattering mode (BSE) with a 20 kV accelerating voltage, 10 mm working distance, and 40 Pa pressure in the chamber constituted the operational conditions for SEM–EDS analysis.

### 2.2.4. Tensiometer

Following the procedure described by Armal et al. [10], a Ramé-Hart Model 210 Tensiometer (Ramé-Hart, Succasunna, NJ, USA) was used to measure static contact angles of the natural stone lithotypes before and after the application of the commercial hydrophobic coatings. The test surfaces were placed horizontally on a sample holder equipped with a dropper, and a pipette was filled with deionized water. The contact angle of each droplet was measured for 3–10 s, with five droplets placed on each natural stone surface. The results were averaged, and the standard deviation was determined. The DROP image software (ver. 3.21.11.0) was used to process the photos and the acquired data.

### 2.2.5. Measurement of Water Vapor Permeability

Following the procedure described by Armal et al. [10], the cup method was applied to measure the water vapor transmission rate [23]. The natural stone mock-ups were oven dried at 60 °C for 24 h and placed in a desiccator for the same amount of time, before

being weighed individually. After being placed in the cup filled with cotton and 1 cm<sup>3</sup> of distilled water, each sample was weighed once again and placed in a FitoClima 600 (Aralab, Rio de Mouro, Portugal) stability test chamber with a temperature of 20 °C and a relative humidity of 40%. The samples were then weighed every 24 h until the difference in weight between measurements became 0.1%, after which, the water vapor permeability values were calculated [10].

#### 2.2.6. Artificial Ageing

Following the procedure described by Armal et al. [10], a QUV-Accelerated Weathering Tester (Q-Lab, College Park, MD, USA), employing the conditions of the standard method of ASTM G154-C7 [24], was used to induce artificial ageing to uncoated and coated natural stone lithotypes and mimic the results of the long-term exposure to real-life outdoor conditions. The mock-ups were subjected to 28 cycles of 12 h each, which included 3:45 h of condensations at 50 °C, 15 min of the spray mode (7 L/min of MilliQ-water) and 8 h of UVA radiation at a 340 nm wavelength at 60 °C (0.75 W/m<sup>2</sup> irradiance).

### 3. Results and Discussion

#### 3.1. Optimization of the Number of Coating Applications

All three commercial coatings were applied at room temperature on the surface of the selected lithotypes by the spray-coating technique. The applications were performed consecutively, but the required drying time for each application was kept in accordance with the manufacturers' recommendations. The effectiveness of the coatings was then assessed for each application via the measurement of the coated lithotypes' static contact angle. Static contact angle measurement is a qualitative method for determining a surface's hydrophobic or hydrophilic properties. A static contact angle greater than 90° indicates an effective hydrophobic surface with poor wetting, while a lower angle, less than 90°, represents a hydrophilic surface with good wetting [25]. Surfaces displaying static water contact angles higher than 150° are considered superhydrophobic [26]. The mean and standard deviation of the static contact angles deriving from the application of five water drops on the uncoated natural stones and the coated lithotypes after each application can be found in Table 2 and are illustrated in Figure 2. The results demonstrate that the three commercial coatings are hydrophobic, imparting water-repellent properties to the selected lithotypes.

In general, CN1 displayed the lowest hydrophobic performance among the commercial coatings tested, while the application of CN2, a colorless VOC-free solution of fluorocarbon polymer, resulted in the highest static contact angles for all three lithotypes (Table 2 and Figure 2). The stable carbon–fluorine bonds and low surface energy of this coating enabled water beading [27,28] and resulted in effective hydrophobicity. Similarly, the application of CN3 resulted in high static contact angles through the combined effects of hydrophobic silane/siloxane and the modified fluorinated compounds present in its constitution. Silane/siloxane coatings penetrate and chemically bond with porous surfaces, forming a stable network, while the modified fluorinated compounds create a water-repellent outer layer [29]. The lower static contact angles achieved when CN1, a potassium methyl siliconate solution, is applied can be attributed to its deep penetration into the porous structure of the natural stone lithotypes, partially wetting their surface. This contrasts with the effects of fluorocarbon-containing coatings, such as CN2 and CN3, which mainly reside on the surface and thus offer superior hydrophobic characteristics [30].



**Table 2.** Static contact angle results obtained for the different coated lithotypes during the optimization of the number of coating applications. Mean and standard deviation were obtained after five measurements.

Lithotypes/Coatings		Limestone (L)		Marble (M)		Granitoid (G)	
		Mean	Stdev	Mean	Stdev	Mean	Stdev
CN1	1st Application	110.9	1.8	113.9	4.1	119.8	3.9
	2nd Application	125.1	2.4	118.6	7.5	127.8	6.4
	3rd Application	125.1	2.6	121.0	8.5	129.4	7.5
	4th Application	126.0	4.0	122.8	9.0	131.1	7.3
CN2	1st Application	132.2	9.5	135.2	7.0	132.6	4.8
	2nd Application	132.8	9.4	135.6	5.4	132.7	4.5
	3rd Application	135.1	7.2	136.8	4.1	134.0	3.2
	4th Application	136.2	6.9	138.0	3.8	135.4	4.2
CN3	1st Application	127.0	3.3	130.0	2.8	133.0	6.2
	2nd Application	136.8	4.3	131.7	4.2	134.1	5.5
	3rd Application	137.4	4.2	132.3	3.8	134.2	5.3
	4th Application	139.2	4.7	133.1	3.7	134.4	5.3

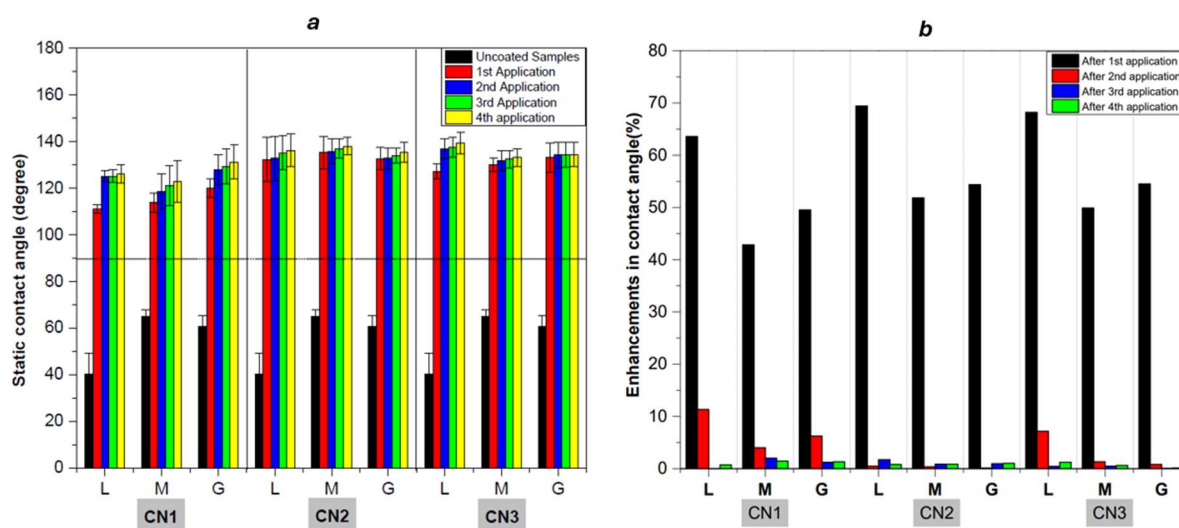


**Figure 2.** (a) Graphical representation of the results of the static contact angles obtained for the different coated lithotypes during the optimization of the number of coating applications; (b) graphical representation of enhancements in contact angle after each coating application.

Nevertheless, as can be seen in Table 2 and Figure 2a, the static contact angles of CN1, CN2, and CN3 increase after the second application, indicating that these hydrophobic coatings become more effective with more applications. However, the increase in the contact angle after the third, and fourth applications is not as significant compared to the first and second applications. As is shown in Figure 2b, the first application of CN1 on limestone resulted in a substantial enhancement in the contact angle, at nearly 65% compared to uncoated limestone. After the second application, the improvement was approximately 12% compared to the first application, and subsequent applications showed progressively smaller increases (0% and 3%). This trend is consistent across other coatings as well, with diminishing enhancements observed after multiple applications, as can be seen in Figure 2b.

An increase in the number of applications most likely results in thicker and more uniform coatings, providing better coverage, which translates into improved water repellency of the coated lithotypes' surface. However, the increased number of applications can also have deleterious effects, as the coatings may become uneven or have diminished adherence to the natural stone surfaces, and cause changes in their aesthetic appearance. In fact, the observation of the natural stone lithotypes after the fourth coating application by SEM revealed that the three commercial coatings display different surface morphologies. As can be seen in Figures 3–5, four applications of CN1 resulted in the formation of a non-uniform, albeit thick coating with cracks and other abnormalities, suggesting a potential lack of compatibility between the coating and the three natural stone substrates. This is further corroborated by elemental mapping performed by SEM–EDS, which clearly shows that elements associated with this commercial hydrophobic coating (silicon and potassium) are not present in the natural stone surfaces visible between the cracks (Figure 6). On the other hand, four applications of commercial coatings CN2 and CN3 resulted in a smoother surface morphology that is generally devoid of roughness or irregularities (Figures 3–5).

Color variations visible to the unaided eye are among the changes in aesthetic appearance that can have a considerable impact on the historical or aesthetic value of natural stone [31]. As such, high-resolution digital microscopy (HIROX) at 30× magnification was employed to assess the visible color hues of the uncoated and coated natural stone lithotypes. Figure 7 displays the photographic record of uncoated substrates and those after the second application of the three coatings on the different natural stone lithotypes. The results indicate that CN2 was the most compatible coating with the selected lithotypes, as no significant aesthetic changes were documented after the second coating application (Figure 7). Unfortunately, this is not the case for both CN1 and CN3, as the second coating application of the first gave rise to the appearance of white spots on the surface of the natural stone lithotypes, which is indicative of severe incompatibility, while the application of CN3 caused visible darkening of the lithotypes' original hue even after only one application (Figure 7). Given these results, the number of applications was limited to one when optimizing the application temperature of the commercial hydrophobic coatings.

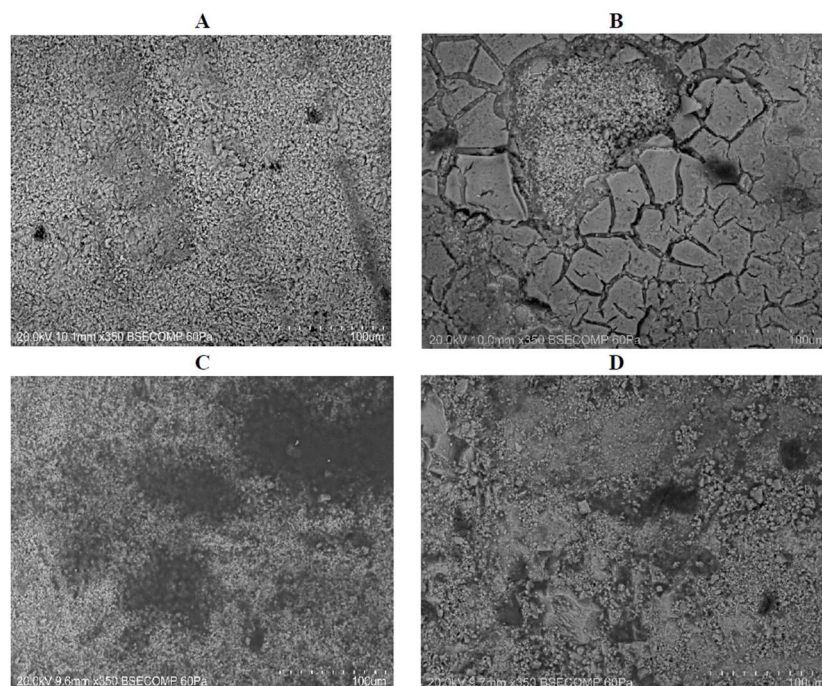


**Figure 3.** SEM image (350×) of the uncoated and coated (with four applications) surface of the selected limestone lithotype. (A) Uncoated; (B) coated with CN1; (C) coated with CN2; (D) coated with CN3.

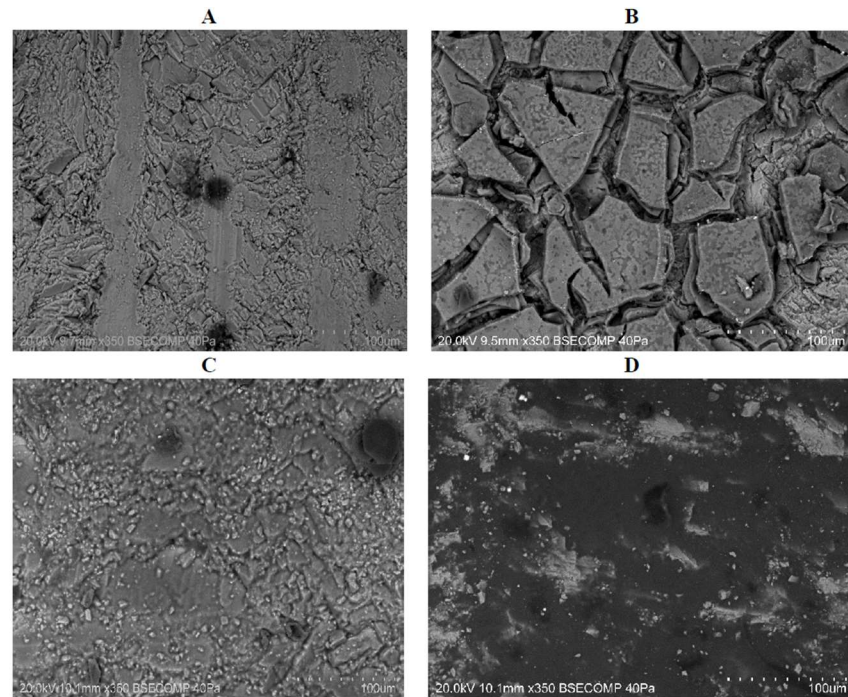


**Figure 4.** SEM image (350×) of the uncoated and coated (with four applications) surface of the selected marble lithotype. (A) Uncoated; (B) coated with CN1; (C) coated with CN2; (D) coated with CN3.

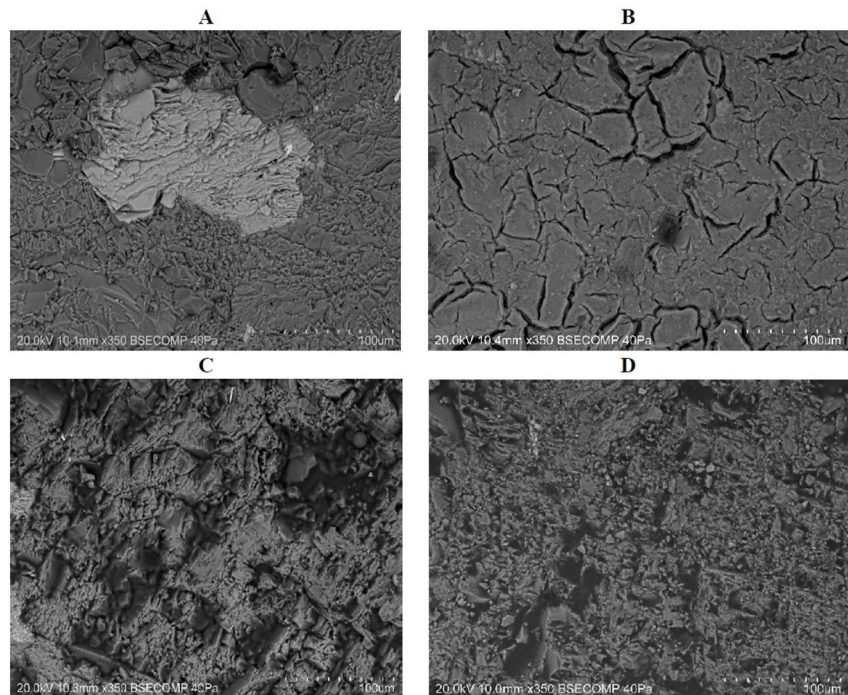


**Figure 5.** SEM image (350×) of the uncoated and coated (with four applications) surface of the selected granitoid lithotype. (A) Uncoated; (B) coated with CN1; (C) coated with CN2; (D) coated with CN3.



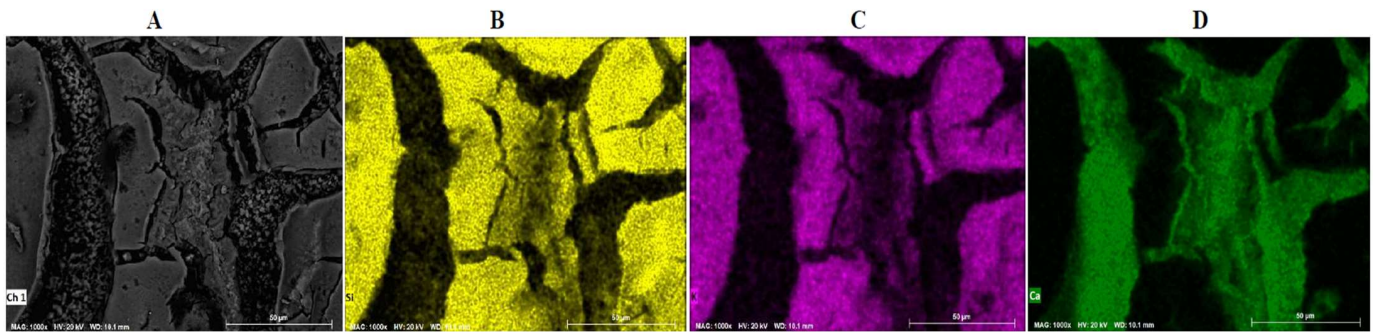


**Figure 6.** Elemental mapping by SEM-EDS of the selected limestone lithotype coated with CN1 (with four applications). (A) Representative BSE image; (B) elemental distribution of silicon (Si); (C) elemental distribution of potassium (K); (D) elemental distribution of calcium (Ca).

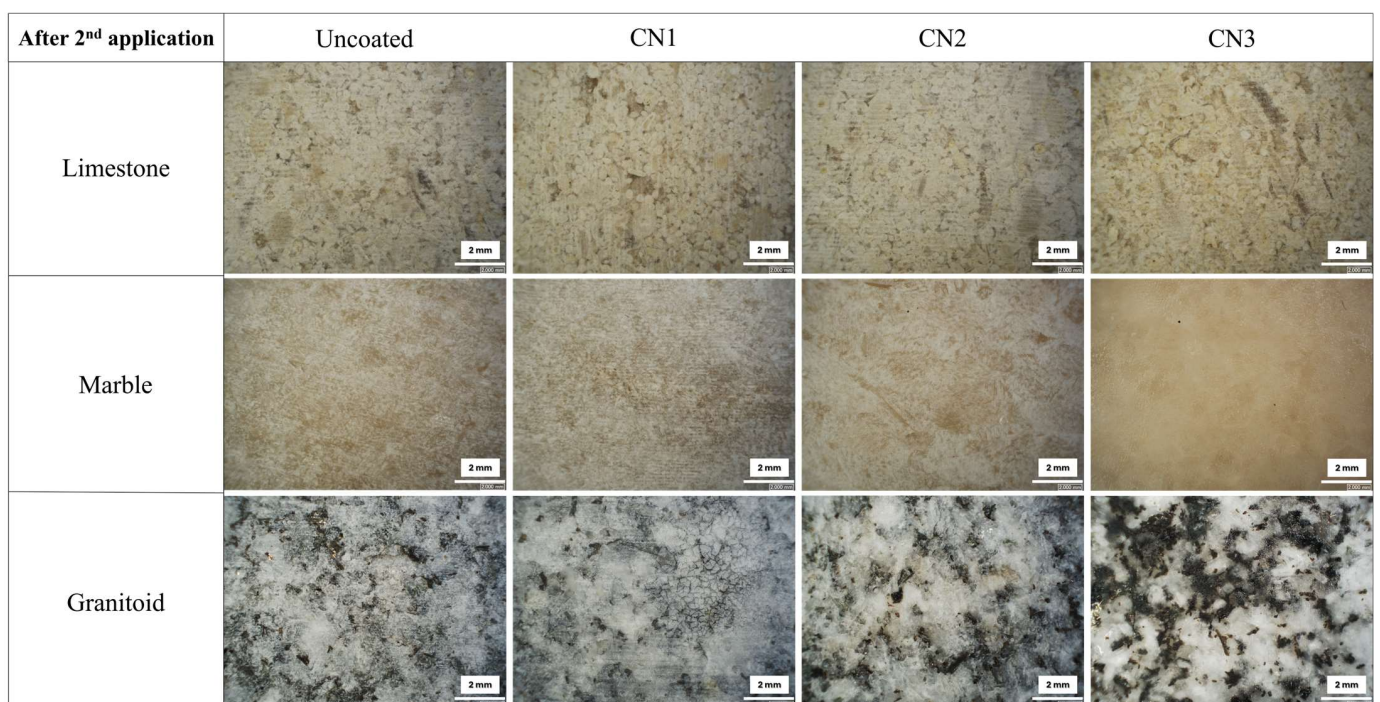


**Figure 7.** High-resolution digital microscope (HIROX) images at 30× magnification of the uncoated substrates and after the second application of studied coatings on the natural stone lithotypes during the assessment of the optimal number of coating applications.

### 3.2. Optimization of the Temperature of Application of Both the Coatings and the Natural Stone Substrates

The three coatings were also applied to the natural stone lithotypes at different temperatures, and with the substrates at different temperatures, to assess the impact of this parameter on their hydrophobic effectiveness. The temperature of the coating and the substrate can affect the thickness and adhesion of the coating. At higher temperatures, the viscosity of the coating can be reduced, allowing it to spread more easily over the surface. However, if the temperature is too high, it can cause the coating to dry too quickly, leading to poor adhesion. The results of the static contact angle measurements are presented in Figure 8 and Table 3.

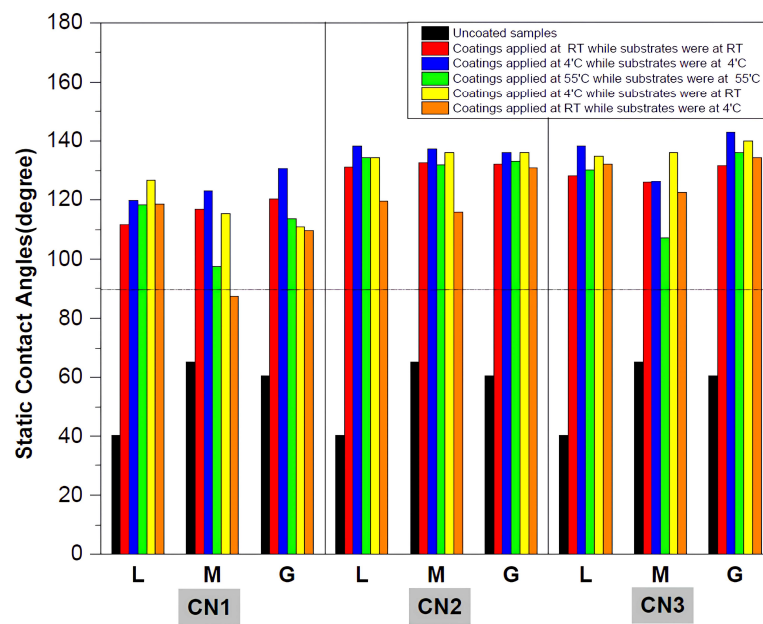


**Figure 8.** Graphical representation of the static contact angle results of the temperature application optimization assessment.

**Table 3.** Static contact angle results of the optimization of the temperature of application of the commercial hydrophobic coatings and natural stone substrates. Mean and standard deviation were obtained after five measurements.

	Lithotypes	Static Contact Angles (Mean $\pm$ Stdev)			
		Uncoated	CN1 Coated	CN2 Coated	CN3 Coated
Coatings applied at room temperature while substrates were at RT	Limestone (L)	40.4 $\pm$ 8.8	110.9 $\pm$ 1.8	132.16 $\pm$ 9.5	127.0 $\pm$ 3.3
	Marble (M)	65.1 $\pm$ 2.8	113.8 $\pm$ 4.1	135.16 $\pm$ 7.0	129.9 $\pm$ 2.8
	Granitoid (G)	60.5 $\pm$ 4.8	119.8 $\pm$ 3.9	132.56 $\pm$ 4.8	133.0 $\pm$ 6.2
Coatings applied at 4 °C while substrates were at 4 °C	Limestone (L)	40.4 $\pm$ 8.8	119.5 $\pm$ 4.3	138.2 $\pm$ 4.3	138.3 $\pm$ 3.5
	Marble (M)	65.1 $\pm$ 2.8	122.8 $\pm$ 6.3	137.2 $\pm$ 5.9	126.0 $\pm$ 4.6
	Granitoid (G)	60.5 $\pm$ 4.8	130.7 $\pm$ 4.6	136.0 $\pm$ 6.5	143.0 $\pm$ 2.2
Coatings applied at 55 °C while substrates were at 55 °C	Limestone (L)	40.4 $\pm$ 8.8	118.2 $\pm$ 3.6	134.5 $\pm$ 2.1	130.2 $\pm$ 2.6
	Marble (M)	65.1 $\pm$ 2.8	97.6 $\pm$ 3.1	131.9 $\pm$ 6.5	107.1 $\pm$ 5.9
	Granitoid (G)	60.5 $\pm$ 4.8	113.6 $\pm$ 1.3	133.0 $\pm$ 3.9	136.1 $\pm$ 4.7
Coatings applied at 4 °C while substrates were at RT	Limestone (L)	40.4 $\pm$ 8.8	126.9 $\pm$ 4.3	134.2 $\pm$ 2.9	134.8 $\pm$ 2.7
	Marble (M)	65.1 $\pm$ 2.8	115.3 $\pm$ 4.2	136.0 $\pm$ 0.8	136.1 $\pm$ 3.4
	Granitoid (G)	60.5 $\pm$ 4.8	110.8 $\pm$ 4.9	136.0 $\pm$ 3.8	139.9 $\pm$ 3.1
Coatings applied at room temperature while substrates were at 4 °C	Limestone (L)	40.4 $\pm$ 8.8	118.3 $\pm$ 6.9	119.4 $\pm$ 4.6	132.2 $\pm$ 1.8
	Marble (M)	65.1 $\pm$ 2.8	87.4 $\pm$ 8.9	115.7 $\pm$ 2.9	122.4 $\pm$ 4.1
	Granitoid (G)	60.5 $\pm$ 4.8	109.7 $\pm$ 3.7	130.8 $\pm$ 3.9	134.4 $\pm$ 2.2

The results obtained indicate that the commercial hydrophobic coatings exhibit increased effectiveness, as evidenced by higher static contact angles, when applied at a temperature of 4 °C to natural stone substrates that are also at 4 °C ( $\approx$ 9% max). The basic reason behind this enhanced effectiveness is likely to be due to the higher viscosity of the hydrophobic coating solution at 4 °C, which makes the spreading of the coating solution slow and promotes the formation of a thick coating layer. This thick coating layer enhances surface roughness and air pockets, resulting in an increase in contact angle and an improvement in water repellency. However, maintaining natural stone surfaces at specific temperatures is not practical or ideal for industrial applications or conservation–restoration interventions, particularly when dealing with large-scale projects associated with built



heritage. Therefore, the application of the coatings at 4 °C onto natural stone substrates maintained at room temperature can be considered the optimal application conditions as it also leads to significantly improved effectiveness (Figure 8 and Table 3).

The presence of potential aesthetic changes on the natural stone lithotypes after the application of the commercial coating solutions under the optimal application temperature conditions was documented using a high-resolution digital microscopy (HIROX) at 30× magnification (Figure 9). In this case, no significant aesthetic changes were observed on either CN1- or CN2-coated lithotypes. Inversely, CN3 caused visible darkening to the original hues of the selected natural stones, particularly to the marble and granitoid lithotypes.

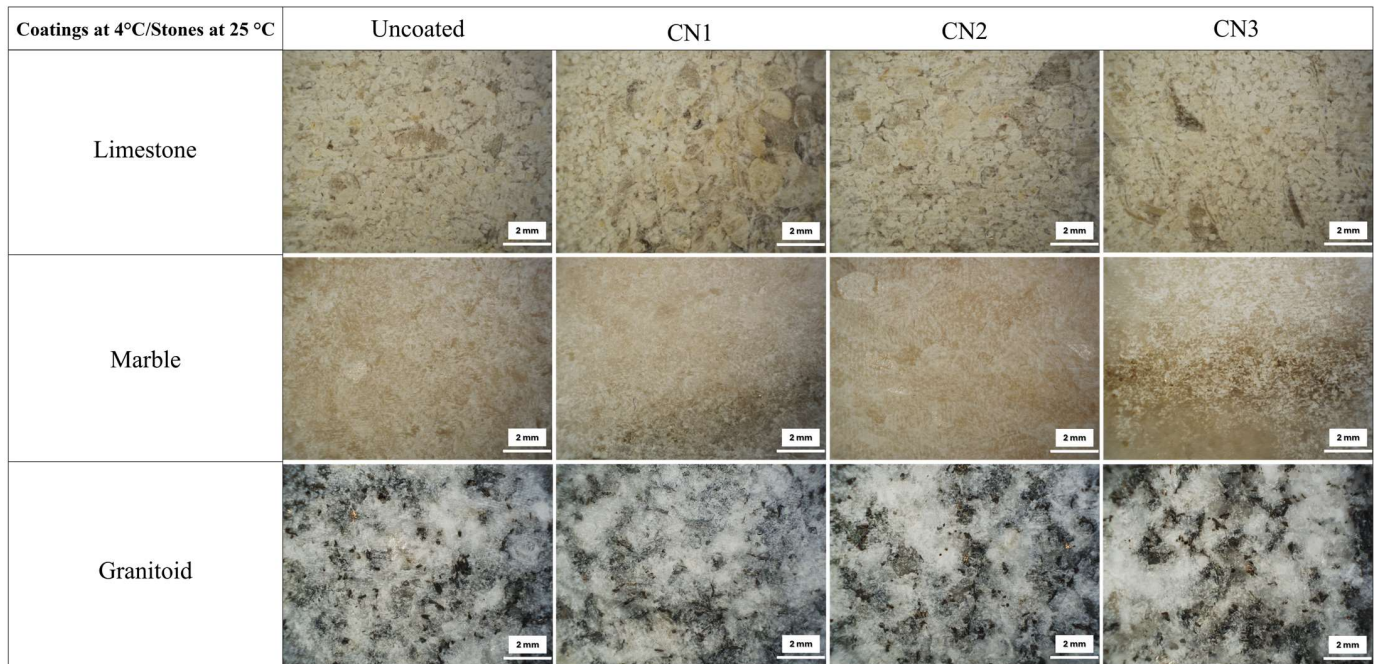


**Figure 9.** High-resolution digital microscope (HIROX) images at 30× magnification of the uncoated substrates and after a single application of studied coatings at 4 °C onto the natural stone lithotypes maintained at room temperature.

After determining the optimal temperature conditions for the application of the three commercial hydrophobic coatings, their durability was assessed by conducting accelerated ageing simulations. In general, coatings that exhibit minimal loss of their properties after accelerated ageing are expected to have greater long-term durability under real-life conditions. Therefore, the static contact angles for the uncoated and coated natural stone lithotypes before and after accelerated ageing were measured to provide insights into the durability of the coatings applied using the predetermined optimal conditions. The results obtained revealed that the hydrophobicity of the uncoated natural stone mock-ups decreased significantly after ageing ( $\approx 63\%$  max) due to the exposure to alternating cycles of UV radiation and moisture in the ageing chamber (Table 4 and Figure 10). The environmental conditions mimicked in the accelerating ageing simulations cause physical and chemical alterations, leading to the formation of microscopic cracks, fissures, and pores that allow water to penetrate natural stones more easily, thereby diminishing their hydrophobicity [32].

In general, accelerated ageing also had a negative impact on the hydrophobicity effectiveness of the coated lithotypes, as evidenced by an almost uniform decrease in the static contact angles after ageing. This is particularly noteworthy in the CN2-coated substrates as the limestone lithotype displays a  $\approx 51\%$  loss on static contact angle values after ageing, so that it effectively loses all hydrophobic properties and becomes hydrophilic, while the coated marble and granitoid lithotypes retain their hydrophobicity (Table 4 and

Figure 10). This difference in behavior between the different coated lithotypes may be related to their different porosities, which may influence the adhesion of the fluorocarbon-polymer-based coating to the substrates. CN2 is, therefore, less durable when applied to porous natural stones, as suggested by the obtained data after the ageing process. In contrast, CN1 and CN3 exhibit greater durability due to their strong adhesion with stone substrates. These coatings work by penetrating the substrate's pores, establishing a strong bond that increases the coating's durability [33]. This enhanced adhesion and penetrability contribute to the coating's resistance to flaking and delamination after accelerated ageing.

**Table 4.** Static contact angle results measured before and after accelerated ageing of natural stone mock-ups with coatings applied at 4 °C on lithotypes maintained at room temperature.

Lithotypes	Static Contact Angles (Mean ± Stdev), Before and After Ageing							
	Uncoated		CN1 Coated		CN2 Coated		CN3 Coated	
	Before	After	Before	After	Before	After	Before	After
L	40.4 ± 8.8	19.3 ± 3.1	126.8 ± 4.3	126.4 ± 4.7	134.2 ± 2.9	64.9 ± 15.4	134.8 ± 2.7	133.2 ± 6.8
M	65.1 ± 2.8	23.8 ± 6.0	115.2 ± 4.2	118.2 ± 21.8	136.0 ± 0.8	127 ± 17.8	136.1 ± 3.4	120.5 ± 10.5
G	60.5 ± 4.8	21.7 ± 9.1	110.7 ± 4.9	123.8 ± 9.7	136.0 ± 3.8	136 ± 3.5	139.9 ± 3.1	137.1 ± 3.5

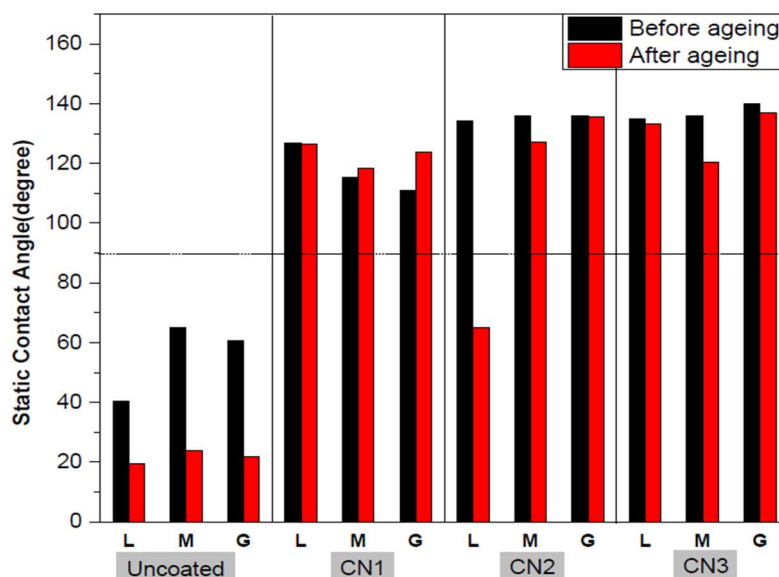


**Figure 10.** Graphical representation of the static contact angle values obtained before and after accelerated ageing of natural stone mock-ups with coatings applied at 4 °C on lithotypes maintained at room temperature.

Maintaining natural stone breathability or intrinsic water vapor permeability is also crucial to ensure good compatibility between a coating and its substrate [32,34]. Water vapor permeability prevents the accumulation of moisture and soluble salts (and the resulting shear stresses) at the interface of the coated zone and the uncoated natural stone substrate below, which can lead to decay [8]. As such, water vapor permeability was assessed for the uncoated natural stone lithotypes and the coated substrates with CN3, as this was previously determined to be the most effective and durable commercial hydrophobic coating. The results displayed in Table 5 indicate that the water vapor permeability value of the limestone lithotype decreased after the application of CN3 and increased after accelerated ageing, while the marble and granitoid lithotypes maintained their breathability both after coating application and after accelerated ageing. This distinct behavior with regard to natural stone breathability may be related to differences in microstructure or open porosity, which are known to cause water vapor permeability values of untreated limestone, marble, and granitoid samples to be significantly different [32].



The water vapor permeability values decreased after the application of CN3 to the limestone lithotype, indicating that the hydrophobic coating reduced its high open porosity. The coating may have also filled the smaller pores to some extent, limiting the pathways available for water vapor to move through the material. The enhancement of the open porosity after accelerated ageing [31] can explain the visible increase in water vapor permeability values after exposure to alternating cycles of UV radiation and moisture, and this might indicate poor compatibility of CN3 when applied to porous carbonated natural stones. On the other hand, the lack of change in water vapor permeability values after the application of CN3 to the marble and granitoid lithotypes, and after being subjected to accelerated ageing, suggests that this commercial hydrophobic coating is compatible with these natural stones.

**Table 5.** Water vapor permeability values (g/m·s·Pa) for each natural stone lithotype before and after the application of CN3 and after accelerated ageing.

Lithotypes	Before Coating Application	After Coating Application	After Accelerated Ageing
L	$6.4 \times 10^{-12}$	$4.0 \times 10^{-12}$	$8.1 \times 10^{-12}$
M	$5.1 \times 10^{-12}$	$5.1 \times 10^{-12}$	$5.1 \times 10^{-12}$
G	$5.5 \times 10^{-12}$	$5.5 \times 10^{-12}$	$5.5 \times 10^{-12}$

Currently, to assess coating durability, there are studies that include an evaluation of exposure to agents under conditions of accelerated ageing and under conditions of natural ageing. The application of accelerated ageing presents several advantages, among which are the greater ease of controlling exposure to deterioration agents [34]. Additionally, by using an accelerated ageing methodology, the results obtained most likely reveal the worst possible scenarios, as extreme exposure conditions are generally used [35]. Thus, this means that it is possible to simulate decades of natural ageing in just a few days of testing in climate chambers, enabling the validation of mathematical models created for stone deterioration simulations [36–38]. This fact is especially relevant when dealing with the preservation of cultural heritage materials, where more prompt action is needed.

#### 4. Conclusions

This study aims at tackling water action on natural stones by optimizing the application procedures of commercial hydrophobic coatings to increase their effectiveness, compatibility, and durability. As such, three commercial solutions with distinct chemical compositions were applied on three different Portuguese natural stone lithotypes that are frequently employed in the production of built heritage, from pre-historic monumental megalithic structures to modern and contemporary buildings.

The results obtained revealed that while more than one application increases coating hydrophobic effectiveness, as evidenced by the rise in static contact angle values, it frequently leads to changes in the aesthetic appearance of natural stone, including whitening and darkening of the substrate's original hues. CN1, a solution based on potassium methyl silicate, is particularly prone to inducing aesthetic changes to natural stones, leading to the formation of macroscopically visible white spots after two applications and resulting in a thick non-uniform coating with cracks and other microscopic abnormalities after four applications.

By measuring the static contact angles of the substrates after applying the commercial coatings at different temperatures on natural stone lithotypes at variable temperatures, it was possible to reach the optimal application conditions. While the commercial hydrophobic coatings exhibit increased effectiveness, as evidenced by higher static contact angles ( $\approx 9\%$  gain), when applied at temperature of  $4\text{ }^{\circ}\text{C}$  to natural stone substrates that are also at  $4\text{ }^{\circ}\text{C}$ , these conditions are not feasible in real life. Therefore, since maintaining natural stone surfaces at specific temperatures is not practical or ideal for industrial purposes or for conservation–restoration interventions, the application of the coatings at  $4\text{ }^{\circ}\text{C}$ , onto natural

stone substrates at room temperature can be considered the optimal application conditions as this also leads to significantly improved hydrophobic effectiveness.

Given the results obtained, the fluorocarbon-polymer-based coating (CN2) and the silane/siloxane-based coating with modified fluorinated additives (CN3) proved to be more effective in imparting hydrophobic properties than that based on potassium methyl silicate (CN1). However, the microstructure of the limestone lithotype proved to be incompatible with CN2, as accelerated ageing simulations revealed that in the long run, porous CN2-coated natural stone substrates tend to become hydrophilic. Water vapor permeability values confirmed that CN3 was the most effective and durable commercial hydrophobic coating tested. CN3 also shows higher compatibility with non-porous natural stone substrates, as its application appears to reduce open porosity, limiting breathability; however, exposure to alternating cycles of UV radiation and moisture under accelerated ageing enhances water vapor permeability while maintaining effective hydrophobicity.

In summary, this study demonstrates that the application conditions of hydrophobic coatings have an impact on their effectiveness, compatibility, and durability. Identifying the optimal application strategies has the potential to revolutionize coating practices across all industries by enhancing the hydrophobic properties of these hybrid solutions. Besides the influence of the coating temperature during its application, other parameters such as curing coating conditions, spray pressure, and optimal solvent choice for dilution must be taken into account in further studies. Moreover, the optimal application conditions achieved in this study are going to be applied to novel and eco-friendly solutions currently under development.

**Author Contributions:** Conceptualization, L.D., S.M. and P.B.; methodology, H.H., L.D., S.M., V.P. and P.B.; validation, H.H., L.D., S.M. and P.B.; formal analysis, H.H.; investigation, H.H.; resources, P.B.; writing—original draft preparation, H.H.; writing—review and editing, L.D., S.M., M.C. and P.B.; visualization, H.H.; supervision, L.D., S.M. and P.B.; project administration, P.B.; funding acquisition, P.B. All authors have read and agreed to the published version of the manuscript.

**Funding:** This research was funded by Fundação para a Ciência e a Tecnologia (FCT) through projects Eco-STONEPROTEC—Eco-friendly superhydrophobic hybrid coatings for STONE PROTECTION (EXPL/CTA-GEO/0609/2021 doi: 10.54499/EXPL/CTA-GEO/0609/2021), UIDB/04449/2020 (doi: 10.54499/UIDB/04449/2020), UIDP/04449/2020 (doi: 10.54499/UIDP/04449/2020), and LA/P/0132/2020 (doi: 10.54499/LA/P/0132/2020). In addition, it was also financed by the European Regional Development Fund and by Sustainable Stone by Portugal—Valorization of natural stone for a digital, sustainable and qualified future”, an action co-financed by the PRR—Recovery and Resilience Plan of the European Union (NextGenerationEU). The financial aid of the European Audiovisual and Culture Executive Agency—EACEA (EMJMD ARCHMAT programme), grant number 599247-EPP-1-2018-1-PT-EPPKA1-JMD-MOB, is also acknowledged.

**Data Availability Statement:** The corresponding author can provide the data from this study upon request.

**Acknowledgments:** The authors express their appreciation to the anonymous companies and Fakolith for their kind contribution of commercial coating samples, which greatly supported the execution of this study.

**Conflicts of Interest:** The authors declare no conflicts of interest.

## References

1. Dani, N. A long continuity: The Ohalo II brush huts (19.5ky) and the dwelling structures in the Natufian and PPNA sites in the Jordan Valley. *Archaeol. Anthropol. Ethnol. Eurasia* **2003**, *13*, 34–48.
2. Atakuman, Ç. Architectural Discourse and Social Transformation During the Early Neolithic of Southeast Anatolia. *J. World Prehistory* **2014**, *27*, 1–42. [[CrossRef](#)]
3. Dolores, P.; Brian, M. The Value of Original natural stone in the Context of Architectural Heritage. *Geosciences* **2016**, *6*, 13. [[CrossRef](#)]
4. Marie, I.; Mujalli, R.O. Quantifying limestone façade performance: An analysis and ranking using logistic model. *J. Build. Rehabil.* **2024**, *9*, 36. [[CrossRef](#)]

5. Dias, A.B.; Pacheco, J.N.; Silvestre, J.D.; Martins, I.M.; de Brito, J. Environmental and Economic Life Cycle Assessment of Recycled Coarse Aggregates: A Portuguese Case Study. *Materials* **2021**, *14*, 5452. [[CrossRef](#)]
6. Strzałkowski, P. Characteristics of Waste Generated in Dimension Stone Processing. *Energies* **2021**, *14*, 7232. [[CrossRef](#)]
7. Ilias, D.C.; Blaga, L.; Iliș, A.; Pereș, A.C.; Caciora, T.; Hassan, T.H.; Hodor, N.; Turza, A.; Taghiyari, H.R.; Barbu-Tudoran, L.; et al. Green Biocidal Nanotechnology Use for Urban Stone-Built Heritage—Case Study from Oradea, Romania. *Minerals* **2023**, *13*, 1170. [[CrossRef](#)]
8. Price, C.A.; Doehne, E. *Stone Conservation: An Overview of Current Research*, 2nd ed.; Getty Publications—Getty Conservation, and CA Institute: Los Angeles, CA, USA, 2011; ISBN 978-1-60606-046-9.
9. Katarzyna, D.; Maciej, T. Analysis of the technical condition of the inner façades of the Donjon at the Kłodzko Fortress. *Bud. Archít.* **2024**, *23*, 87–100. [[CrossRef](#)]
10. Armal, F.; Dias, L.; Mirão, J.; Pires, V.; Sitzia, F.; Martins, S.; Costa, M.; Barrulas, P. Chemical Composition of Hydrophobic Coating Solutions and Its Impact on Carbonate Stones Protection and Preservation. *Sustainability* **2023**, *15*, 16135. [[CrossRef](#)]
11. Charola, A.E.; Wendler, E. An overview of the water-porous building materials interactions. *Restor. Build. Monum.* **2015**, *21*, 55–65. [[CrossRef](#)]
12. Kazancı, N.; Ozlem, A.; Ozlem, A. Stones of Göbeklitepe, SE Anatolia, Turkey: An Example of the Shaping of Cultural Heritage by Local Geology Since the Early Neolithic. *Geoheritage* **2022**, *14*, 57. [[CrossRef](#)]
13. Ševčík, R.; Machotová, J.; Zářybnická, L.; Mácová, P.; Viani, A. Aqueous polyacrylate latex nanodispersions used as consolidation agents to improve mechanical properties of Prague sandstone. *J. Cult. Herit.* **2023**, *62*, 412–421. [[CrossRef](#)]
14. Margherita, Z.; Mazzon, G.; Bertolacci, L.; Carzino, R.; Zendri, E.; Athanassiou, A. Stone Sustainable Protection and Preservation Using a Zein-Based Hydrophobic Coating. *Prog. Org. Coat.* **2021**, *159*, 106434. [[CrossRef](#)]
15. Horie, C.V. *Materials for Conservation*, 2nd ed.; Routledge: London, UK, 2010. [[CrossRef](#)]
16. Mehdi, S.-S.; Ershad-Langroudi, A. Polymeric Coatings for Protection of Historic Monuments: Opportunities and Challenges. *J. Appl. Polym. Sci.* **2009**, *112*, 2535–2551. [[CrossRef](#)]
17. Ruffolo, S.A.; La Russa, M.F. Nanostructured Coatings for Stone Protection: An Overview. *Front. Mater.* **2019**, *6*, 147. [[CrossRef](#)]
18. Sierra-Fernandez, A.; Gomez-Villalba, L.; Rabanal, M.; Fort, R. New Nanomaterials for Applications in Conservation and Restoration of Stony Materials: A Review. *Mater. De Construcción* **2017**, *67*, 107. [[CrossRef](#)]
19. Cappelletti, G.; Fermo, P.; Camiloni, M. Smart Hybrid Coatings for natural stones Conservation. *Prog. Org. Coat.* **2015**, *78*, 511–516. [[CrossRef](#)]
20. Manoudis, P.N.; Tsakalof, A.; Karapanagiotis, I.; Zuburtikudis, I.; Panayiotou, C. Fabrication of Super-Hydrophobic Surfaces for Enhanced Stone Protection. *Surf. Coat. Technol.* **2009**, *203*, 1322–1328. [[CrossRef](#)]
21. Pires, V.; Mirão, J.; Sitzia, F.; Lisci, C.; Duarte, J.; Dias, L.; Alves, T.; Lopes, L.; Martins, R. *Advanced Technologies for Natural Stone | Inovstone 4.0-Important Results from a Research Project on Natural Stone Construction Materials Selection and Performance Analysis*; Rehabend: Andalucía, Spain, 2022; pp. 1337–1350, ISBN 978-840942252-4. Available online: <http://www.rehabend.unican.es> (accessed on 23 June 2024).
22. Aditya, K.; Nanda, D. Chapter 3—Methods and Fabrication Techniques of Superhydrophobic Surfaces. In *Superhydrophobic Polymer Coatings*; Elsevier: Amsterdam, The Netherlands, 2019; pp. 43–75. [[CrossRef](#)]
23. *ASTM E96/E96M-14*; Standard Test Methods for Water Vapor Transmission of Materials. ASTM International: Kansas City, MO, USA, 2014.
24. *ASTM G154C7*; Resistance of a Nonmetallic Material to Simulated Sunlight and Moisture Exposure. ASTM International: West Conshohocken, PA, USA, 2006.
25. Erbil, H.Y. Evaporation of pure liquid sessile and spherical suspended drops. *Adv. Colloid Interface Sci.* **2012**, *170*, 67–86. [[CrossRef](#)]
26. Li, X.-M.; Reinhoudt, D.; Crego-Calama, M. What Do We Need for a Superhydrophobic Surface? A Review on the Recent Progress in the Preparation of Superhydrophobic Surfaces. *Chem. Soc. Rev.* **2007**, *36*, 1350–1368. [[CrossRef](#)]
27. Sumit, P.; Dixit, P.; Chattopadhyay, S. Superhydrophobic Surfaces: Insights from Theory and Experiment. *J. Phys. Chem. B* **2020**, *124*, 1323–1360. [[CrossRef](#)]
28. McKeen, L.W. *Fluorinated Coatings and Finishes Handbook: The Definitive User's Guide*, 2nd ed.; Elsevier Science: Amsterdam, The Netherlands, 2015.
29. Wu, L.; Baghdachi, J. *Functional Polymer Coatings: Principles, Methods, and Applications*; John Wiley & Sons: Hoboken, NJ, USA, 2015.
30. Kronlund, D. Chemical Engineering of Surface Coatings for Natural Stones. Master's Thesis, Åbo Akademi University, Åbo, Finland, 2017.
31. Mariateresa, L.; Masieri, M.; Morelli, A.; Pipoli, M.; Frigione, M. Oleo/Hydrophobic Coatings Containing Nanoparticles for the Protection of Stone Materials Having Different Porosity. *Coatings* **2018**, *8*, 429. [[CrossRef](#)]
32. Andreotti, S.; Franzoni, E.; Fabbri, P. Poly(hydroxyalkanoate)s-Based Hydrophobic Coatings for the Protection of Stone in Cultural Heritage. *Materials* **2018**, *11*, 165. [[CrossRef](#)] [[PubMed](#)]
33. Li, L.; Li, B.; Dong, J.; Zhang, J. Roles of Silanes and Silicones in Forming Superhydrophobic and Superoleophobic Materials. *J. Mater. Chem.* **2016**, *4*, 13677–13725. [[CrossRef](#)]
34. Rivas, T.; Prieto, B.; Silva, B. Permeability to Water Vapour in Granitic Rocks. Application to the Study of Deleterious Effects of Conservation Treatments. *Build. Environ.* **2001**, *36*, 239–246. [[CrossRef](#)]

35. Schulz, U. *Accelerated Testing: Nature and Artificial Weathering in the Coatings Industry*; Vincentz Network: Hannover, Germany, 2009; ISBN 978-3-86630-908-1.
36. Bellopede, R.; Zichella, L.; Marini, P.; Luodes, N.M. Natural stone decay: Artificial ageing tests versus natural weathering. In *Conserving Cultural Heritage*, 1st ed.; Mosquera, M., Almoraima Gil, M.L., Eds.; CRC Press: London, UK, 2018; ISBN 9781315158648.
37. Timoncini, A.; Brattich, E.; Bernardi, E.; Chiavari, C.; Tositti, A. Safeguarding outdoor cultural heritage materials in an ever-changing troposphere: Challenges and new guidelines for artificial ageing test. *J. Cult. Herit.* **2023**, *59*, 190–201. [[CrossRef](#)]
38. Saba, M.; Quiñones-Bolaños, E.E.; Barbosa López, A.L. A review of the mathematical models used for simulation of calcareous stone deterioration in historical buildings. *Atmos. Environ.* **2018**, *180*, 156–166. [[CrossRef](#)]

**Disclaimer/Publisher’s Note:** The statements, opinions and data contained in all publications are solely those of the individual author(s) and contributor(s) and not of MDPI and/or the editor(s). MDPI and/or the editor(s) disclaim responsibility for any injury to people or property resulting from any ideas, methods, instructions or products referred to in the content.